Journal of Applied Physics

RESEARCH ARTICLE | JULY 12 2023

Influence of Si(111) substrate off-cut on AlN film crystallinity grown by magnetron sputter epitaxy

Katrin Pingen; Stefan Neuhaus; Niklas Wolff; Lorenz Kienle; Agnė Žukauskaitė; Elizabeth von Hauff; Alexander M. Hinz

Journal of Applied Physics 134, 025304 (2023)
https://doi.org/10.1063/5.0156659

View Online

Export Citation

CrossMark

02 August 2023 10:01:43

Journal of Applied Physics | ARTICLE | pubs.aip.org/aip/jap

Influence of Si(111) substrate off-cut on AlN film crystallinity grown by magnetron sputter epitaxy

Cite as: J. Appl. Phys. **134**, 025304 (2023); doi: 10.1063/5.0156659
Submitted: 3 May 2023 · Accepted: 27 June 2023 ·
Published Online: 12 July 2023

View Online

Export Citation

CrossMark

Katrin Pingen,[1,2,a)] Stefan Neuhaus,[1,2] Niklas Wolff,[3,4] Lorenz Kienle,[3,4] Agnė Žukauskaitė,[1,2] Elizabeth von Hauff,[1,2] and Alexander M. Hinz[1,2,a)]

AFFILIATIONS

[1]Fraunhofer Institute for Organic Electronics, Electron Beam and Plasma Technology FEP, Winterbergstraße 28, Dresden D-01277, Germany
[2]Institute of Solid State Electronics (IFE), Technische Universität Dresden, Mommsenstraße 15, Dresden D-01069, Germany
[3]Synthesis and Real Structure, Department of Material Science, Kiel University, Kaiserstraße 2, Kiel D-24143, Germany
[4]Kiel Nano, Surface and Interface Science (KiNSIS), Kiel University, Christian-Albrechts-Platz 4, Kiel D-24118, Germany

[a)]**Authors to whom correspondence should be addressed:** katrin.pingen@fep.fraunhofer.de and alexander.martin.hinz@fep.fraunhofer.de

ABSTRACT

The increasing demand for More than Moore devices requires epitaxy technology to keep up with the discovery and deployment of new semiconductors. An emerging technology for cost-effective, device-quality growth is magnetron sputter epitaxy, though detailed studies on the process itself remain scarce. Here, we report an extensive study on the correlation between the substrate off-cut and film quality in AlN-on-Si heteroepitaxy. Controlled reactive pulsed magnetron sputtering is used to grow epitaxial AlN(0001) films on *in situ* Ar plasma etched off-cut Si(111) substrates with growth rates above 1.5 nm/s. Substrate off-cut angles in the range of 0.02°–0.30° are investigated and precisely determined by high-resolution x-ray diffraction. Structural examination of the AlN films is carried out by transmission electron microscopy and high-resolution x-ray diffraction. The AlN/Si interface is well-defined and two types of AlN domains with epitaxial relationships are observed. The formation of secondary rotation domains deteriorates the crystal quality substantially. Substrates with small off-cuts, ideally no off-cut substrates, appear to be crucial for suppressing the formation of secondary domains and further result in a better overall crystal quality of AlN films. We discuss this effect in relation to the AlN/Si interface, the substrate pre-treatment, and nucleation.

© 2023 Author(s). All article content, except where otherwise noted, is licensed under a Creative Commons Attribution (CC BY) license (http://creativecommons.org/licenses/by/4.0/). https://doi.org/10.1063/5.0156659

02 August 2023 10:01:43

I. INTRODUCTION

AlN thin films are ubiquitous in epitaxial film stacks for a wide range of group III-nitride optoelectronics and power electronic devices. These devices typically require films with high crystal quality and smooth surface morphology to achieve high efficiencies.[1–4] Growing such films heteroepitaxially on Si(111) is advantageous because of the low cost and good availability of large area Si substrates, combined with silicon's high thermal conductivity and simple integration into Si-based process chains. Established deposition methods, such as metalorganic vapor phase epitaxy (MOVPE), are suitable to grow device-quality, heteroepitaxial AlN films on Si substrates.[5–8] However, magnetron sputter epitaxy (MSE) offers many advantages for AlN deposition. MSE is a high-rate process that can be applied at a large-scale for cost-effective and high throughput deposition. Furthermore, MSE reduces the required growth temperature by several hundred degrees Celsius compared to MOVPE enabling lower thermal stresses in films and direct integration with Si-complementary metal-oxide-semiconductor technology.[9,10] Combining MSE with the *in situ* pre-treatment method of Ar plasma etching, the process further reduces the production cost compared to other established pre-treatment methods, such as wet chemical etching. To achieve AlN film quality that is sufficient for device applications, the governing parameters of the AlN MSE process first need to be identified and optimized. While the impact of other MSE process parameters, such as growth temperature and process pressure, has been investigated,[11–14] the

influence of the substrate off-cut angle on the film quality of AlN grown by MSE has not yet been the focus of earlier studies. In heteroepitaxial growth, it is well-established that the substrate off-cut can be used to manipulate the properties of the epitaxial films. This ranges from improving the annihilation of dislocations in epitaxial lateral overgrowth to the suppression of antiphase domains and the elimination of rotated domains.[15,16] To our knowledge, our report is the first study on the influence of the off-cut angle in AlN-on-Si (111) MSE.

II. EXPERIMENTS

AlN films are grown on n-type Si(111) substrates from various suppliers (SIEGERT WAFER GmbH, Siltronic AG, ABC GmbH) by controlled reactive pulsed magnetron sputtering. *In situ* Ar plasma etching is applied to remove the surface oxides of the substrates prior to AlN deposition. The Ar plasma etch rate is 0.09 nm/s for SiO_2 and approximately 7 nm is removed directly before AlN growth. All AlN films are grown in a high-vacuum chamber with a base pressure of 1×10^{-5} Pa equipped with a double ring magnetron (DRM) developed by Fraunhofer FEP.[17] The DRM is operated in a bipolar pulse mode with a duty cycle of 60%.[14] The total process pressure is 0.5 Pa with an argon–nitrogen gas mixture at a growth temperature of 800 °C. A constant target voltage is maintained by regulating the nitrogen flow with a proportional-integral-derivative control loop enabling growth rates above 1.5 nm/s, which is one order of magnitude higher than typical MOVPE rates.[18] All investigated AlN films have a thickness of 560 ± 10 nm, as determined by spectroscopic ellipsometry (J. A. Woollam M-2000) combined with a Cauchy-model fit. The crystal structure of the AlN films and the substrate off-cut of the Si (111) substrates are examined by high-resolution x-ray diffraction (XRD, Bruker D8 Discover equipped with Goebel mirror and LynxEye XE detector). Figure 1 shows the schematic geometry of the XRD setup with three angular rotations ω, φ, and ψ. To determine the substrate off-cut, ω scans of Si 111 reflection at four different φ angles with a spacing of 90° are measured for each sample similar to the method described by M. A. G. Halliwell and S. J. Chua.[19] X-ray reflectometry is used for the alignment of the sample surface by correcting the position of the reflected beam to the measured maximum intensity by a given incidence angle for ω and ψ

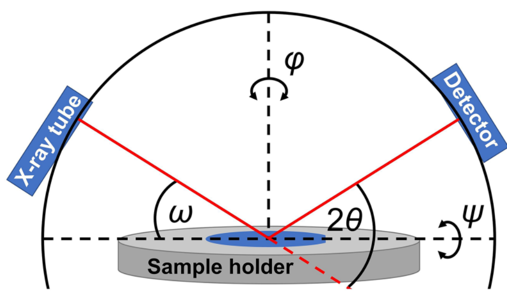

FIG. 1. Schematic geometry of the XRD setup showing the three angular rotations ω, φ, and ψ; the incident angle ω; and the diffracted angle 2θ.

movements. After the alignment of the surface normal to the goniometer axis, shifts in the position of Si 111 Bragg reflection can be attributed to the substrate off-cut. The off-cut angle can be split into two components attributed to the off-cut direction. By using the relative φ positions 0°, 90°, 180°, and 270° for ω scans, the off-cut angle α can be calculated as

$$\alpha = \sqrt{((\omega_{\varphi=0^\circ} - \omega_{\varphi=180^\circ})\ /\ 2)^2 + ((\omega_{\varphi=90^\circ} - \omega_{\varphi=270^\circ})\ /\ 2)^2}\ .$$

The error in the off-cut angle is estimated for each sample by comparing the absolute values of deviation from the theoretical ω position of the Si 111 reflection for φ scans that are 180° apart, respectively. The average error of the substrate off-cut measurements amounts to $\Delta\alpha = 0.015°$ for the investigated sample population of 18 samples with substrate off-cuts in the range of $\alpha = 0.02°–0.30°$.

The crystal quality of the AlN films is evaluated by the full width at half maximum of XRD rocking curves (ω-FWHM) of AlN 0002 (c-axis) and AlN $10\bar{1}1$ reflections. Further investigation is carried out on cross-sectional AlN samples by high-resolution transmission electron microscopy (HRTEM, FEI Tecnai F30 G^2 STWIN, 300 kV) prepared for observation along the Si [112] zone axis that is coincident with AlN $[10\bar{1}0]$ orientation. The surface morphology and polarity of selected samples are analyzed by atomic force microscopy and piezoresponse force microscopy, respectively (AFM and PFM, NX20 Park Systems).

III. RESULTS AND DISCUSSION

A. Structural analysis

We begin by examining the crystal quality of the AlN films, and in a second step, we use the evaluation of the crystal quality to correlate it to the substrate off-cut. While $2\theta/\omega$ XRD scans (not presented here) show c-axis-oriented growth for all AlN films, the ω scans reveal striking differences between the AlN films. Although all AlN films are grown under identical deposition conditions, the ω-FWHMs of AlN 0002 and AlN $10\bar{1}1$ reflections range from 1.0° to 1.2° and 1.5° to 3.5°, respectively. This variation in crystal quality can be attributed to the formation of a secondary crystal domain. Depicted in Fig. 2 are representative φ scans of the AlN $10\bar{1}1$ reflection of four different AlN samples. Epitaxially grown AlN films are expected to show a sixfold symmetry following the (111) Si-substrate orientation ideally matching the φ scan of sample 1 in Fig. 2. However, φ scans reveal that some AlN films exhibit a secondary domain with an in-plane orientation that is shifted by 30° with respect to the primary domain, as observed for samples 2–4 in Fig. 2. For some samples, the volume fraction of the secondary domain can even become dominant over the primary domain (Fig. 2, samples 3 and 4).

In the absence of secondary domains, the epitaxial nature of the single domain AlN film is confirmed by HRTEM measurements shown in Fig. 2. The selected area electron diffraction pattern observed along the Si [112] zone axis [Fig. 3(a)] depicts a $[10\bar{1}0]$ single crystalline-like spot pattern for the AlN film indicating a high structural coherence and a fixed in-plane orientation, following the threefold symmetry of the Si(111) substrate. The cross-sectional HRTEM image of the AlN/Si interface depicted in Fig. 1(b) clearly shows the direct, oriented growth of AlN without

02 August 2023 10:01:43

© Author(s) 2023

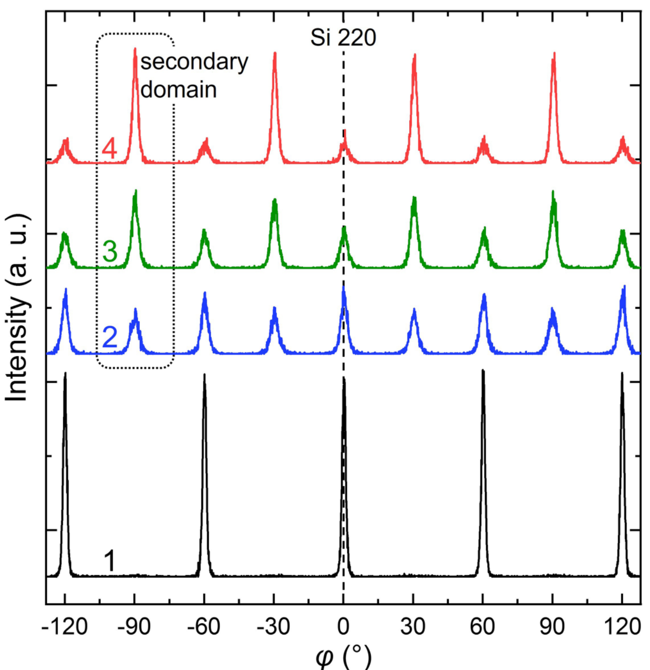

FIG. 2. XRD φ scans of AlN $10\bar{1}1$ reflections of four different AlN samples 1–4 with the Si 220 substrate reflection marked as a reference.

intermediate transition layers at the interface. The results of φ scans can be combined with selected area electron diffraction data for the identification of two orientation domains with epitaxial relationships of AlN $[2\bar{1}\bar{1}0]\|$Si [110] and AlN $[10\bar{1}0]\|$Si [110] for primary and secondary domains, respectively. A visualization of epitaxial relationships is given in Fig. S1 in the supplementary material.

To get a better understanding of the impact of the secondary domains on the films, their contribution to the total film volume is estimated from φ scans. The area under each reflection in the φ scans is determined from a Voigt profile fit and averaged over all corresponding reflections of the primary domain A^{I} and the secondary domain A^{II}. The secondary domain fraction $f_{A^{II}}$ is then determined as $f_{A^{II}} = A^{II} \times 100/(A^{I} + A^{II})$ for each sample. In Fig. 4, the ω-FWHM of (a) 0002 and (b) $10\bar{1}1$ AlN reflections are plotted against the secondary domain fraction. To evaluate the in-plane crystal quality, the ω-FWHM of the $10\bar{1}1$ AlN reflection of the dominant domain type, i.e., the one with a domain fraction $f_A > 50$ vol. %, is depicted in Fig. 4(b). From this analysis, two subsets with distinct in-plane orientation as well as out-of-plane orientation are derived from the total sample population. The first subset with a large volume fraction of secondary domains $f_{A^{II}} > 40$ vol. % and the second one with a small volume fraction of secondary domains $f_{A^{II}} < 5$ vol. %. The correlation of the out-of-plane crystal orientation with the secondary domain fraction, as shown in Fig. 4(a), indicates the presence of a maximum of the mosaic tilt component at intermediate volume fractions close to $f_{A^{II}} \sim 20$ vol. %. Since the high symmetry of the c-axis of the

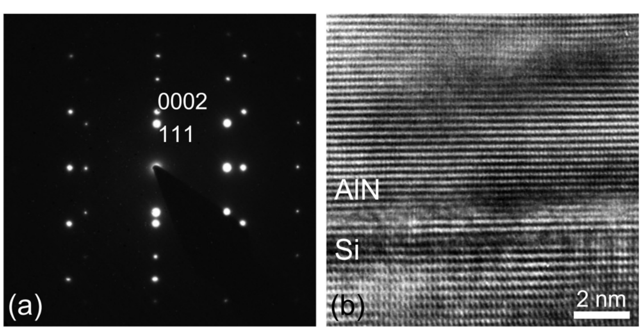

FIG. 3. (a) Selected area electron diffraction pattern observed along the Si [112] zone axis with Si 111 and AlN 0002 diffraction spots indexed and (b) cross-sectional HRTEM image of the AlN/Si interface.

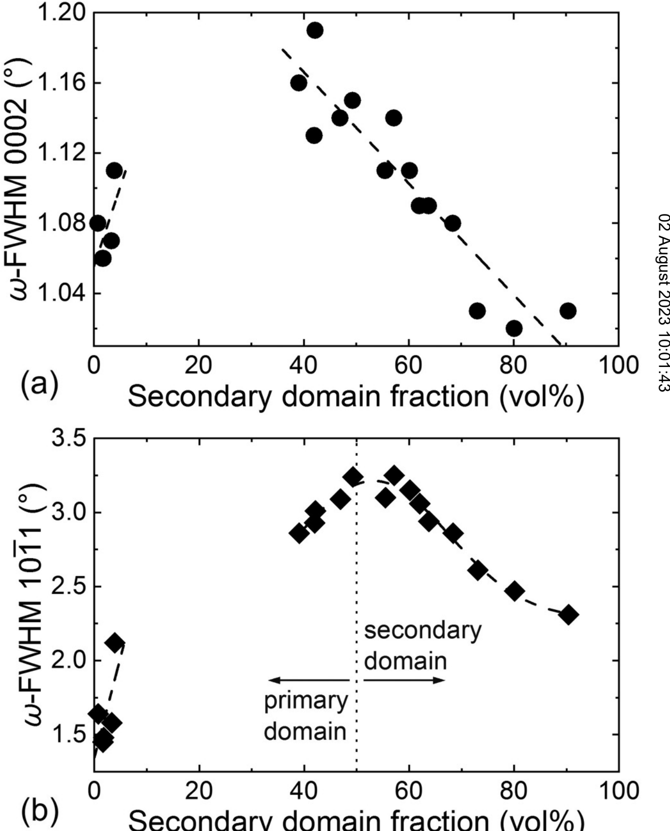

FIG. 4. ω-FWHM of XRD rocking curves of (a) AlN 0002 reflection and (b) AlN $10\bar{1}1$ reflection as a function of the secondary domain fraction. In (b), the ω-FWHM of the $10\bar{1}1$ AlN reflection of the dominant domain type, i.e., the one with a domain fraction >50 vol. % is evaluated. The sample population consists of two subsets centered around 2and 59 vol. % of secondary domain fraction. The dashed lines are a guide to the eye.

02 August 2023 10:01:43

© Author(s) 2023

hexagonal wurtzite structure is a driving force for epitaxial growth,[20] a high tilt is unfavorable and might prohibit secondary domain fractions in an intermediate range. To minimize the tilt, the defect structure in the grown AlN films may rearrange itself in a way that secondary domain fractions between 10 and 30 vol. % do not occur. In detail, the lowest out-of-plane ω-FWHM values occur if either the primary or the secondary domain is dominantly present. The presence of both domains in a balanced ratio leads to an undesirable overall drop of AlN film quality. The analysis of in-plane mosaicity is depicted in Fig. 4(b) and shows high values of ω-FWHM for samples with equally distributed domain fractions in the range of 40 vol. % > $f_{A^{II}}$ > 70 vol. %. If we take the ω-FWHM of the $10\bar{1}1$ reflection as a measure of the twist component of the AlN film mosaicity, the data in Fig. 4(b) indicate that films with a low secondary domain volume fraction have a lower overall twist component. Since the secondary domains are misaligned by 30° in-plane compared to primary domains, an increased overall twist is expected. Additional dislocations with an edge component are required to accommodate the secondary domains in the film, leading to an overall increase in the in-plane ω-FWHM. The absolute change of the overall twist as a consequence of the formation of secondary domains is much larger compared to the tilt.

B. Correlation with the substrate off-cut

As a next step, we correlate the variations in crystal quality with the substrate off-cut. Therefore, the secondary domain fraction is plotted as a function of the substrate off-cut in Fig. 5(a). Once more, the two subsets of the sample population centered around 2 and 59 vol. % of secondary domain fraction are identified. Neither of the subsets shows any correlation with the substrate off-cut. However, considering the general occurrence rather than the inherent volume fraction of the secondary domain, a correlation of the substrate off-cut and the formation of the secondary domains are revealed. Figure 5(b) shows the statistical occurrence of secondary domains, i.e., the fraction of samples that have a significant amount (>5 vol. %) of secondary domains as a function of the substrate off-cut. The off-cut has been divided into bins with a width of 0.05° for this analysis. The distribution in Fig. 5(b) suggests that a small, ideally no substrate off-cut is important for suppressing the formation of secondary domains. From the experimental results, this effect is interpreted in relation to the AlN/Si interface, the substrate pre-treatment and nucleation. Since hexagonal (0001) AlN has a large lattice mismatch of 19% with the Si(111) surface, three-dimensional growth is expected. We also assume that each domain type originates during nucleation since antiphase boundaries are energetically unfavorable in bulk AlN. Ar plasma etching is carried out just before AlN growth and leaves, in contrast to wet chemical etching combined with annealing steps,[21] an uncontrolled Si surface, where no single reconstruction of the Si(111) surface can be expected. Locally the Si surface is either atomically flat or exhibits steps typically along the $\langle\bar{1}10\rangle$ or $\langle11\bar{2}\rangle$ direction with a step height of 3.14 Å.[22,23] The primary domain with the epitaxial relationship of AlN $[2\bar{1}\bar{1}0]$||Si $[11\bar{2}]$ and the secondary domain with the epitaxial relationship of AlN $[10\bar{1}0]$||Si $[11\bar{2}]$ may favor different nucleation sites. Higher substrate off-cuts result in an increased number of step terraces on the Si(111) surface. The 0001 AlN

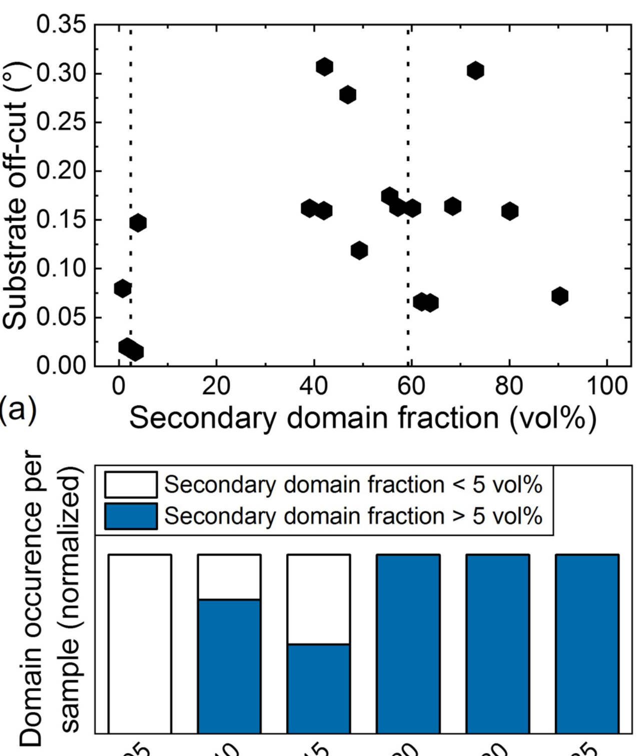

FIG. 5. (a) Si(111) substrate off-cut as a function of the AlN secondary domain fraction. The dotted lines at 2 and 59 vol. % of secondary domain fraction mark the center of the two subsets of the sample population. (b) Statistical occurrence of secondary domain fractions above and below 5 vol. % in AlN films as a function of the Si(111) substrate off-cut.

02 August 2023 10:01:43

planes are parallel to the 111 Si planes on each terrace. The *c* unit cell parameter of AlN is 4.98 Å introducing a small local rotation to enable the continuity of the 0001 AlN planes at Si steps. The secondary domain with the epitaxial relationship of AlN $[10\bar{1}0]$||Si $[11\bar{2}]$ may be a better fit at Si steps. Si substrate steps are known to cause discontinuous growth in epitaxy for several material systems.[24,25] On bulk-like surfaces, the AlN $[2\bar{1}\bar{1}0]$||Si $[11\bar{2}]$ primary domain may be energetically favorable due to the partial coincidence of the surface bond directions of the Si substrate and of AlN nuclei. If separated islands with either one of the two orientations nucleate and continue growing, the boundaries between the differently oriented domains need to be accompanied by dislocations.[22] Additional dislocations deteriorate the crystal quality which we see for the samples with a balanced domain ratio. The Si surface is defined by the surface treatment and MSE process parameters. Although HRTEM does not indicate nitridation and a sharp AlN/Si interface is observed, the Si surface preparation is inherently uncontrolled. MSE is a non-equilibrium process and different

© Author(s) 2023

process parameters govern the kinetic energy that the substrate surface is exposed to during nucleation. However, nucleation may only define the initial formation of secondary domains but not the eventual fraction of the secondary domains, since during growth of 500 nm AlN some of the nucleated secondary domains can be overgrown. A more thorough investigation of the nucleation and growth mechanisms of the AlN films is necessary to further investigate this effect but is beyond the scope of this contribution.

As the presence of secondary domains likely obscures the influence of the substrate off-cut on crystal quality, only samples dominantly consisting of a primary domain are a reliable indication for the particular influence of the off-cut. In Fig. 6, the impact of the substrate off-cut on crystal quality is depicted for samples with a secondary domain fraction of <50 vol. %. The out-of-plane orientation [Fig. 6(a)] as well as the in-plane orientation [Fig. 6(b)] exhibit a nearly linear decrease in the ω-FWHM with decreasing substrate off-cut. However, the in-plane orientation is much more sensitive to variations in the substrate off-cut. The corresponding data indicate that the overall tilt and twist components in the films can be significantly decreased by using a smaller substrate off-cut. Thus, using a small substrate off-cut does not only appear to be beneficial for suppressing the formation of secondary domains, but also for increasing the overall crystal quality of the grown AlN films.

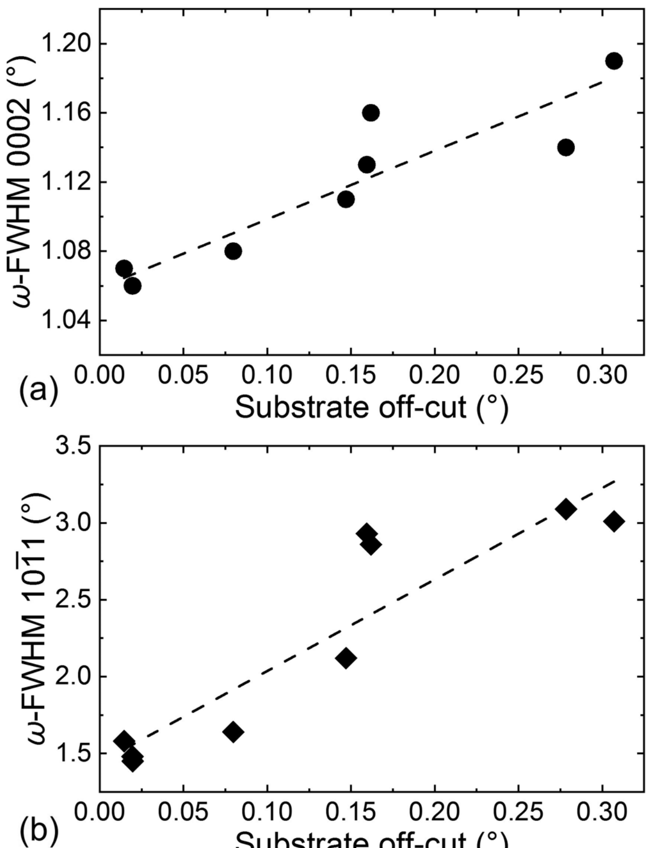

FIG. 6. ω-FWHM of XRD rocking curves of (a) AlN 0002 reflection and (b) AlN $10\bar{1}1$ reflection as a function of the substrate off-cut. The dashed lines are a guide for the eye.

C. Surface and polarity

Apart from having sufficient crystal quality, thin films for device fabrication also require smooth, ideally atomically flat, surfaces. Based on the marked impact of the substrate off-cut and the presence of secondary domains on the crystal quality, one might expect that the surface morphology is similarly affected. However, this does not seem to be the case. AFM measurements of selected samples show no impact of the substrate off-cut on surface morphology of the AlN films. The surface exhibits a pebble-like morphology, typical for sputtered films with a columnar microstructure, with a root mean square roughness of 2.4 ± 0.2 nm calculated from $2 \times 2\,\mu\text{m}^2$ AFM scans for all examined samples. PFM shows no impact of the substrate off-cut on the polarity of the AlN samples. All examined AlN samples are N-polar. As the polarity of AlN films is often manipulated by altering the chemical composition of the substrate, for example, through nitridation, this suggests that the driving force for forming secondary domains is different from the mechanisms resulting in a polarity inversion. The AFM and PFM images can be found as Figures S2 and S3 in the supplementary material, respectively.

IV. CONCLUSIONS

In summary, the impact of the substrate off-cut on sputtered AlN(0001)/Si(111) films is investigated using high-resolution XRD techniques. The epitaxial nature of the AlN films is confirmed by HRTEM and two domains with epitaxial relationships are observed. Lower substrate off-cuts suppress the formation of secondary domains that substantially deteriorate the crystal quality and independent of secondary domains lead to AlN films with higher crystal quality. Substrates with ideally no off-cut exhibit the most favorable results. Therefore, in the context of the investigated high-rate MSE process, it is crucial to carefully select substrates to inhibit the formation of secondary domains and promote the growth of high-quality AlN films. This effect is interpreted in relation to the AlN/Si interface, the substrate pre-treatment, and nucleation. Other factors that promote the formation of secondary domains still have to be identified. This will be the subject of a more detailed future study.

02 August 2023 10:01:43

SUPPLEMENTARY MATERIAL

See the supplementary material for Figure S1 showing a visualization of the epitaxial relationships and Figures S2 and S3 showing additional AFM and PFM data, respectively.

ACKNOWLEDGMENTS

The authors thank Dr. O. Zywitzki, Dr. T. Modes, and R. Belau for their contribution to the sample analysis. Dr. N. Wolff would like to acknowledge funding from the DFG in the framework of (CRC1261) project A6. S. Neuhaus would like to acknowledge funding from the project HiPERFORM (ECSEL grant agreement

© Author(s) 2023

No 783174). K. Pingen and Dr. A. M. Hinz would like to acknowledge funding through the project ForMikro-GaNESIS (FKZ: 16ES1089K) and the Fraunhofer Internal Programs under Grant No. Attract 061-601007.

AUTHOR DECLARATIONS

Conflict of Interest

The authors have no conflicts to disclose.

Author Contributions

Katrin Pingen: Conceptualization (equal); Data curation (equal); Formal analysis (equal); Investigation (equal); Methodology (equal); Validation (equal); Visualization (equal); Writing – original draft (equal); Writing – review & editing (equal). **Stefan Neuhaus:** Investigation (equal); Software (equal); Writing – review & editing (equal). **Niklas Wolff:** Formal analysis (equal); Visualization (equal); Writing – review & editing (equal). **Lorenz Kienle:** Writing – review & editing (equal). **Agnė Žukauskaitė:** Supervision (equal); Writing – review & editing (equal). **Elizabeth von Hauff:** Supervision (equal); Writing – review & editing (equal). **Alexander M. Hinz:** Formal analysis (equal); Funding acquisition (equal); Project administration (equal); Supervision (equal); Validation (equal); Visualization (equal); Writing – review & editing (equal).

DATA AVAILABILITY

The data that support the finding of this study are available from the corresponding author upon reasonable request.

REFERENCES

[1]L. Shen, S. Heikman, B. Moran, R. Coffie, N.-Q. Zhang, D. Buttari, I. P. Smorchkova, S. Keller, S. P. DenBaars, and U. K. Mishra, IEEE Electron Device Lett. **22**, 457 (2001).
[2]F. A. Ponce and D. P. Bour, Nature **386**, 351 (1997).
[3]U. K. Mishra, P. Parikh, and Y.-F. Wu, Proc. IEEE **90**, 1022 (2002).
[4]M. Kneissl, T. Kolbe, C. Chua, V. Kueller, N. Lobo, J. Stellmach, A. Knauer, H. Rodriguez, S. Einfeldt, Z. Yang, N. M. Johnson, and M. Weyers, Semicond. Sci. Technol. **26**, 014036 (2011).
[5]F. Semond, P. Lorenzini, N. Grandjean, and J. Massies, Appl. Phys. Lett. **78**, 335 (2001).
[6]C. J. Zollner, A. Almogbel, Y. Yao, B. K. SaifAddin, F. Wu, M. Iza, S. P. DenBaars, J. S. Speck, and S. Nakamura, Appl. Phys. Lett. **115**, 161101 (2019).
[7]A. Dadgar, A. Strittmatter, J. Bläsing, M. Poschenrieder, O. Contreras, P. Veit, T. Riemann, F. Bertram, A. Reiher, A. Krtschil, A. Diez, T. Hempel, T. Finger, A. Kasic, M. Schubert, D. Bimberg, F. A. Ponce, J. Christen, and A. Krost, Phys. Status Solidi C **0**(6), 1583–1606 (2003).
[8]D. Zhu, D. J. Wallis, and C. J. Humphreys, Rep. Prog. Phys. **76**, 106501 (2013).
[9]F. Hörich, R. Borgmann, J. Bläsing, G. Schmidt, P. Veit, F. Bertram, J. Christen, A. Strittmatter, and A. Dadgar, J. Cryst. Growth **571**, 126250 (2021).
[10]N. Izyumskaya, V. Avrutin, K. Ding, Ü. Özgür, H. Morkoç, and H. Fujioka, Semicond. Sci. Technol. **34**, 093003 (2019).
[11]A. Dadgar, F. Hörich, R. Borgmann, J. Bläsing, G. Schmidt, P. Veit, J. Christen, and A. Strittmatter, Phys. Status Solidi A **220**(8), 2200609 (2022).
[12]T. Watanabe, J. Ohta, T. Kondo, M. Ohashi, K. Ueno, A. Kobayashi, and H. Fujioka, Appl. Phys. Lett. **104**, 182111 (2014).
[13]A. Prabaswara, J. Birch, M. Junaid, E. A. Serban, L. Hultman, and C.-L. Hsiao, Appl. Sci. **10**, 3050 (2020).
[14]S. Neuhaus, H. Bartzsch, S. Cornelius, K. Pingen, A. Hinz, and P. Frach, Surf. Coat. Technol. **429**, 127884 (2022).
[15]J. Enslin, A. Knauer, A. Mogilatenko, F. Mehnke, M. Martens, C. Kuhn, T. Wernicke, M. Weyers, and M. Kneissl, Phys. Status Solidi A **216**, 1900682 (2019).
[16]T. Suski, E. Litwin-Staszewska, R. Piotrzkowski, R. Czernecki, M. Krysko, S. Grzanka, G. Nowak, G. Franssen, L. H. Dmowski, M. Leszczynski, P. Perlin, B. Łucznik, I. Grzegory, and R. Jakieła, Appl. Phys. Lett. **93**, 172117 (2008).
[17]H. Bartzsch, P. Frach, K. Goedicke, and C. Gottfried, Surf. Coat. Technol. **120–121**, 723 (1999).
[18]A. Dadgar, A. Krost, J. Christen, B. Bastek, F. Bertram, A. Krtschil, T. Hempel, J. Bläsing, U. Haboeck, and A. Hoffmann, J. Cryst. Growth **297**, 306 (2006).
[19]M. A. G. Halliwell and S. J. Chua, J. Cryst. Growth **192**, 456 (1998).
[20]K. Dovidenko, S. Oktyabrsky, J. Narayan, and M. Razeghi, J. Appl. Phys. **79**, 2439 (1996).
[21]A. Ishizaka and Y. Shiraki, J. Electrochem. Soc. **133**, 666 (1986).
[22]A. Bourret, A. Barski, J. L. Rouvière, G. Renaud, and A. Barbier, J. Appl. Phys. **83**, 2003 (1998).
[23]R. S. Becker, J. A. Golovchenko, E. G. McRae, and B. S. Swartzentruber, Phys. Rev. Lett. **55**, 2028 (1985).
[24]J. Wollschläger, Appl. Phys. A: Mater. Sci. Process. **75**, 155 (2002).
[25]S. Borisova, J. Kampmeier, M. Luysberg, G. Mussler, and D. Grützmacher, Appl. Phys. Lett. **103**, 081902 (2013).

02 August 2023 10:01:43

© Author(s) 2023